

NACA TN No. 1813

8259

# NATIONAL ADVISORY COMMITTEE FOR AERONAUTICS

TECHNICAL NOTE

No. 1813

A STUDY OF FLOW CHANGES ASSOCIATED WITH AIRFOIL  
SECTION DRAG RISE AT SUPERCRITICAL SPEEDS

By Gerald E. Nitzberg and Stewart Crandall

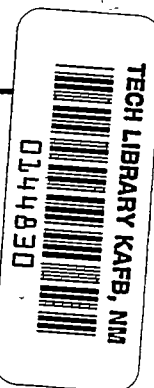
Ames Aeronautical Laboratory  
Moffett Field, Calif.



Washington

February 1949

AF 1813  
TECHNICAL NOTE  
AFL 2511



9-144



## NATIONAL ADVISORY COMMITTEE FOR AERONAUTICS

---

TECHNICAL NOTE NO. 1813

---

## A STUDY OF FLOW CHANGES ASSOCIATED WITH AIRFOIL

## SECTION DRAG RISE AT SUPERCRITICAL SPEEDS

By Gerald E. Nitzberg and Stewart Crandall

## SUMMARY

A study of experimental pressure distributions and section characteristics for several moderately thick airfoil sections was made. A correlation appears to exist between the drag-divergence Mach number and the free-stream Mach number for which sonic velocity occurs at the airfoil crest, the chordwise station at which the airfoil surface is tangent to the free-stream direction. It was found that, since the Mach number for which sonic velocity occurs at the airfoil crest can be estimated satisfactorily by means of the Prandtl-Glauert rule, a method is provided whereby the drag-divergence Mach number of an airfoil section at a given angle of attack can be estimated from the low-speed pressure distribution and the airfoil profile. This method was used to predict with a reasonable degree of accuracy the drag-divergence Mach number of a considerable number of airfoil sections having diverse shapes and a wide range of thickness-chord ratios.

The pressure distributions and section force characteristics of several moderately thick airfoil sections at Mach numbers above the drag-divergence Mach number were analyzed. Some of the characteristics of the flow over these airfoils at supercritical Mach numbers are discussed.

## INTRODUCTION

The first intensive efforts to develop airfoil sections suitable for high-subsonic-speed applications were directed toward obtaining sections with the highest possible critical speeds. It was reasoned that, if the first occurrence of local sonic velocity on the airfoil surface could be delayed to higher free-stream Mach numbers, then, the

adverse lift and drag changes associated with supercritical speeds could be delayed. However, experimental measurements show that the onset of these adverse effects is not directly related to the critical Mach number. For some types of airfoil sections the drag rises rapidly as soon as the free-stream Mach number exceeds the critical; whereas for other types no appreciable drag rise occurs until the Mach number of the free stream is considerably above the critical.

No adequate method has been presented for predicting the free-stream Mach numbers at which the various supercritical flow changes occur. The purpose of the present report is to investigate these flow changes for two-dimensional transonic flow past conventional and low-drag airfoil sections. The investigation is based primarily on a systematic analysis of experimental data for airfoil sections of 15-percent-chord thickness. Although this thickness is greater than is generally desirable for use at high speeds, it has the advantage that airfoil-shape effects are less likely to be masked by boundary-layer effects.

#### SYMBOLS

$\alpha$	airfoil section angle of attack
$c$	airfoil chord
$c_d$	airfoil section drag coefficient
$c_l$	airfoil section lift coefficient
$M$	ratio of local velocity to local velocity of sound
$M_p$	free-stream Mach number at which sonic velocity is first reached at airfoil crest
$M_{cr}$	critical Mach number of airfoil section (free-stream Mach number at which local sonic velocity is first reached on airfoil surface)
$M_d$	drag-divergence Mach number (Mach number at which slope of curve of drag coefficient versus Mach number attains a value of 0.10)
$M_o$	ratio of free-stream velocity to free-stream velocity of sound

$M_s$	shock-stall Mach number (free-stream Mach number at which boundary-layer separation first occurs at rear of airfoil)
$P$	pressure coefficient $\left( \frac{p-p_o}{q_o} \right)$
$p$	local static pressure on the airfoil surface
$p_o$	static pressure of the free stream
$q_o$	dynamic pressure of the free stream
$x$	chordwise distance from airfoil leading edge
$(x/c)_\beta$	airfoil crest (chordwise station at which the airfoil surface is tangent to the direction of the free stream)

#### DETERMINATION OF DRAG-DIVERGENCE MACH NUMBER

As the free-stream Mach number is increased through the critical value, the first abrupt change in airfoil section characteristics, for an airfoil section at a moderate angle of attack, is the rapid increase in drag coefficient. For some airfoil sections at certain angles of attack this drag rise begins at the critical Mach number; whereas for other cases it does not begin until the free-stream Mach number is considerably greater than the critical. Some high-speed pressure distributions and section characteristics (reference 1) for the NACA 65<sub>2</sub>-215 ( $\alpha = 0.5$ ), 66<sub>2</sub>-215 ( $\alpha = 0.6$ ), 0015, 23015, and 4415 airfoil sections have been studied in an attempt to determine the flow changes which are associated with the appearance of this more or less abrupt drag rise. In order to supplement these data, simultaneous pressure distributions and schlieren pictures of the flow around the NACA 23015 airfoil section were obtained in the Ames 1- by 3-1/2-foot high-speed wind tunnel. Before considering the specific problem of the flow changes associated with the appearance of the supercritical drag rise, the data for this airfoil section will be discussed in detail.

Measurements at Supercritical Speeds for  
NACA 23015 Airfoil at  $2^\circ$  Incidence

Lift- and drag-coefficient variation with Mach number for the NACA 23015 airfoil section at  $2^\circ$  angle of attack is presented in figure 1. For this section at  $2^\circ$  angle of attack, the critical Mach number, which is the free-stream Mach number at which sonic velocity is first attained at some point on the airfoil surface, is 0.59. The first abrupt change in the section characteristics occurs at a somewhat higher free-stream Mach number, and consists of a drag-coefficient increase from the low-speed value. That free-stream Mach number at which the rate of increase of drag coefficient with Mach number equals 0.1 is defined, as in reference 1, as the drag-divergence Mach number. The free-stream Mach number at which the experimental pressure distribution first indicates the presence of marked boundary-layer thickness is termed the shock-stall Mach number. More detailed information about the supercritical flow changes over the NACA 23015 airfoil section at  $2^\circ$  angle of attack is obtained from the schlieren pictures and corresponding pressure distributions presented in figure 2. At a Mach number of 0.60 there is a small region of supersonic flow which contains alternate expansion and compression regions, as can be seen from the schlieren picture. The pressure distribution resembles that for subcritical speeds. When the free-stream Mach number is increased to 0.65, the drag-divergence Mach number, a strong shock wave appears near the airfoil crest (the chordwise station at which the surface is tangent to the free-stream direction) but no change in the boundary-layer thickness is apparent in the schlieren photograph. From the pressure distribution, it is seen that at the airfoil crest the local velocity is greater than sonic. Thus, sonic velocity is reached at the airfoil crest at a Mach number between 0.60 and 0.65. In figures 2(b), 2(c), and 2(d) the terminal shock wave stands close to the chordwise station at which the local pressure coefficient corresponds to sonic velocity. At 0.70 and 0.73 free-stream Mach numbers, there is a marked thickening of the boundary layer ahead of the shock wave, which is located aft of the airfoil crest. This rapid thickening of the boundary layer appears to start at the airfoil crest. The pressure distribution over the rear of the upper surface of the airfoil for free-stream Mach numbers of 0.70 and 0.73 resembles that for the smaller Mach numbers and thus gives no indication of the presence of a thick boundary layer. However, the schlieren photograph for a free-stream Mach number of 0.73 does indicate the presence of a thick boundary layer over the rear of the airfoil upper surface. The drag coefficient at this Mach number is about 0.04, which is comparable to the drag coefficient for low-speed maximum lift at the same Reynolds number.

Figure 3(a) shows the variation of pressure coefficient with Mach

number at several chordwise stations on the upper surface of the NACA 23015 airfoil section at  $2^\circ$  angle of attack. Here the airfoil crest is at the 22-percent-chord station on the upper surface. At points well forward of the crest, that is, at the 5- and 10-percent-chord stations, the local pressure coefficient ceases to fall with increasing Mach number somewhat before the drag-divergence Mach number. Closer to the crest, at the 15- and 20-percent-chord stations, the smooth decrease in pressure coefficient with increasing Mach number continues until the free-stream Mach number reaches the value for drag divergence. After the drag-divergence Mach number is exceeded, the pressure coefficients at points ahead of the airfoil crest rise in such a manner as to maintain virtually constant local Mach numbers. For points immediately behind the airfoil crest, the 25-, 30-, and 40-percent-chord stations on the upper surface, the local Mach number does not rise smoothly from subsonic to supersonic values since, at each chordwise position, as the shock wave moves past, there is an abrupt rise from a local Mach number slightly less than unity to a value greater than unity. However, at each of these chordwise positions, the free-stream Mach number for which the local velocity becomes sonic agrees quite well with the value obtained by assuming the pressure-coefficient variation with free-stream Mach number to follow the Prandtl-Glauert rule. For points far back on the upper surface, the 60- and 85-percent-chord stations, at a free-stream Mach number of about 0.73, there is a marked increase in the rate of fall of local pressure coefficient with increasing free-stream Mach number. The presence of a thick boundary layer over the rear of the airfoil is thus indicated by the pressure distribution and 0.73 is termed the shock-stall Mach number. A similar change in the variation of local pressure coefficient with free-stream Mach number occurs for the entire lower surface of the airfoil (fig. 3(b)) at a free-stream Mach number somewhat below 0.73. This marked decrease of local pressure coefficient with increasing free-stream Mach number resembles the pressure-distribution changes associated with increasing boundary-layer separation as the lift coefficient of an airfoil approaches maximum lift at low speeds. It is interesting to note (fig. 1) that, for the NACA 23015 airfoil section at  $2^\circ$  angle of attack, the marked decrease in lift coefficient with increasing Mach number which begins at a Mach number of about 0.7 is primarily a result of the rapid decrease of pressure coefficients on the lower surface of the airfoil (fig. 3(b)).

Measurements at Supercritical Speeds for NACA 23015  
Airfoil at Various Angles of Attack

In figure 4 are presented the variations of pressure coefficient

with Mach number at various chordwise stations for the NACA 23015 airfoil section at several angles of attack. The local pressure-coefficient variation with Mach number at the crest location, for each angle of attack shown in figure 4, is denoted by a solid curve. It is seen that for each angle of attack the drag-divergence Mach number differs only slightly from the free-stream Mach number at which sonic velocity occurs at the airfoil crest. As the Mach number is increased beyond the value for drag divergence there is a rise in pressure coefficient with Mach number at points ahead of the crest; and, at least up to a Mach number of 0.8, this pressure-coefficient variation with free-stream Mach number is such as to maintain practically constant local Mach numbers.

### Origin of Drag Rise

The relation between the pressure-distribution changes noted for the NACA 23015 airfoil section and the supercritical drag rise will now be considered. At approximately the drag-divergence Mach number, there is established over the forward portion of the upper surface of the NACA 23015 airfoil a Mach number distribution which remains relatively unchanged with some further increase of free-stream Mach number. In figure 3, it is seen that, while pressure coefficients ahead of the crest are becoming less negative, pressure coefficients at points well aft of the airfoil crest become more negative as the Mach number increases above that for drag divergence. This combination of pressure changes produces a rising pressure drag which appears to be the primary factor in the supercritical drag rise. It should be pointed out that the negatively increasing pressure coefficients aft of the airfoil crest may result from two different causes: the rearward growth of the supersonic region, and marked boundary-layer thickening. Both of these causes may be present, as for example, on the NACA 23015 airfoil section at  $2^\circ$  angle of attack.

### Prediction of the Drag-Divergence Mach Number

In the preceding sections the flow changes over the NACA 23015 airfoil section at supercritical speeds were considered for various angles of attack. It was noted that increasing the free-stream Mach number produces no abrupt changes in the airfoil section characteristics until the supersonic region extends behind the airfoil crest. When this occurs, the drag begins to rise rapidly with increasing Mach number. Figure 5 shows that for the NACA 23015 airfoil section the calculated and experimental values of  $M_g$ , the Mach number at which sonic velocity occurs at the airfoil crest, are in reasonable

agreement with measured values of the drag-divergence Mach number. The experimental value of  $M_p$  at a given angle of attack was obtained from a plot of the experimentally determined pressure coefficient at the airfoil crest as a function of free-stream Mach number. The free-stream Mach number at which this curve passed through a value corresponding to a local Mach number of unity was termed  $M_{p_{exp}}$ . The calculations consisted of determining the free-stream Mach number at which sonic velocity was reached at the airfoil crest by applying the Prandtl-Glauert rule to the low-speed experimental pressure coefficient at the airfoil crest. For comparison, there are also shown in figure 5 the critical Mach number  $M_{cr}$  and the shock-stall Mach number  $M_s$  at which marked boundary-layer thickening or separation is first indicated by negatively increasing pressure coefficients over the tail of the airfoil. It is seen that these latter two curves are not closely related to drag divergence. Similar data for several other 15-percent-thick airfoil sections are presented in figure 6. For all these cases, the Mach number for which the velocity at the crest is calculated to be sonic is close to the drag-divergence Mach number evaluated from the section drag characteristics.

The five airfoil sections, for which drag-divergence has been related to the occurrence of sonic velocity at the airfoil crest, are relatively thick sections. Since no rigorous causal relation between these phenomena has been demonstrated, it is desirable to investigate the applicability of the method for thinner airfoil sections. In figure 7, calculated values of  $M_p$  and measured drag-coefficient variation with Mach number are presented for a large number of airfoil sections. The calculations consisted of applying the Prandtl-Glauert compressibility correction to the low-speed pressure distributions in order to determine the Mach number at which sonic velocity occurs at the airfoil crest. The drag data for the 6-percent-thick symmetrical sections were obtained from reference 2 and the data for the cambered 6-series airfoils were measured in the Ames 1- by 3-1/2-foot high-speed wind tunnel on 6-inch-chord models which spanned the 1-foot dimension of the tunnel. It is seen that for each of these airfoil sections a useful measure of the free-stream Mach number at which drag divergence occurs is that Mach number at which the calculated velocity at the airfoil crest is sonic.

## DISCUSSION OF FLOW CHARACTERISTICS AT MACH NUMBERS

### ABOVE THE DRAG-DIVERGENCE MACH NUMBER

In the previous sections of the report some characteristics of the supercritical flow past airfoil sections at subsonic free-stream



speeds have been pointed out. These characteristics will be considered further in this section of the report. Attention has already been directed to the aft boundary of the supersonic region. In figure 8, the variation of the chordwise extent of the region of supersonic flow over the NACA 23015 airfoil section is shown as a function of Mach number. It is seen that the fore and aft boundaries shift until the drag-divergence Mach number is reached. The forward sonic point remains relatively fixed for some further increase in free-stream Mach number while the aft sonic point continues to move rearward of the airfoil crest  $(x/c)_p$ . At Mach numbers above that for drag divergence the rear sonic point lies close to the position of the shock wave, as determined from the schlieren photographs. Reference 3 shows that the chordwise location of the shock wave can be altered by scale effects. The question therefore arises as to whether these data, obtained at a test Reynolds number of about 2 million, apply at larger Reynolds numbers. Unpublished German pressure-distribution data, for the NACA 23015 airfoil section at  $0^\circ$  incidence and a Reynolds number of about 5 million, are shown for comparison in figure 8. The chordwise extent of the supersonic region is nearly the same for both sets of experimental data. However, as can be seen from figure 4, there is some small difference between the variation of local pressure coefficients with Mach number at 2 million and 5 million Reynolds number.

The appearance of a fixed chordwise location of the forward sonic point at subsonic free-stream Mach numbers above that for drag-divergence is to be expected since, as has been noted for the NACA 23015 airfoil section, the pressure-coefficient variation at these Mach numbers appears to be such as to maintain an approximately constant local Mach number distribution over that portion of the airfoil surface ahead of the crest. The location of the forward sonic point for each of the airfoils of reference 1 is shown as a function of Mach number in figure 9. The farthest forward station at which pressures were measured for that report was the 2.5-percent-chord station so that the angles of attack which could be considered were limited to those for which the sonic point was near or behind this station. It appears (fig. 9) that the forward sonic point is fixed at Mach numbers above the drag-divergence Mach number only for those cases for which the sonic point lies between the 2.5- and 15-percent-chord stations. When the sonic point is outside of this region at the drag-divergence Mach number there is some movement of the sonic point with further increase in Mach number. This movement appears to be greatest for the two low-drag airfoil sections which have, at a fixed Mach number, large variation of sonic point location with angle of attack.

The experimental pressure distribution for each of the cases considered in figure 9 reveals that at Mach numbers above that of drag divergence the maximum local Mach number occurs near the airfoil crest. This phenomenon is probably characteristic of moderately thick airfoil sections only; but, for these cases, it suggests the possibility of predicting the peak pressure coefficient. In figure 10 the experimental local Mach number distribution over the NACA 23015 airfoil section at  $2^\circ$  angle of attack is shown for several free-stream Mach numbers greater than that of drag divergence. The Prandtl-Meyer theoretical Mach number distribution for this airfoil is shown for comparison; although, of course, this theory is not valid for a supersonic region of limited extent normal to the airfoil chord. It is seen that a close approximation to the experimental local Mach number distribution can be obtained by taking one-half of the Prandtl-Meyer Mach number increment per degree of surface turning. Figure 11 shows that, for the airfoil sections considered in figure 9, a useful approximation to the local Mach number at the airfoil crest for Mach numbers above that for drag divergence is obtained by using one-half the Mach number increment predicted by the Prandtl-Meyer theory. In these calculations the sonic point was assumed to be that at the drag-divergence Mach number.

#### CONCLUDING REMARKS

A good measure of the free-stream Mach number at which the abrupt supercritical drag rise begins has been shown to be that Mach number at which sonic local velocity occurs at the airfoil crest. This fact provides a method for calculating the drag-divergence Mach number. The method consists of determining the free-stream Mach number at which sonic velocity occurs at the airfoil crest by applying the Prandtl-Glauert compressibility factor to the low-speed pressure distribution. The usefulness of this method is demonstrated by comparing the calculated drag-divergence Mach number with that determined experimentally for a wide variety of airfoil shapes.

The mixed subsonic and supersonic flow fields which exist at supercritical speeds are extremely difficult to treat mathematically. The general considerations of this report are no substitute for such an analysis, but they do present a simplified picture of this complex type of flow which should be useful in planning further studies.

Ames Aeronautical Laboratory,  
National Advisory Committee for Aeronautics,  
Moffett Field, Calif.

## REFERENCES

1. Graham, Donald J., Nitzberg, Gerald E., and Olson, Robert N.:  
A Systematic Investigation of Pressure Distributions at High  
Speeds Over Five Representative NACA Low-Drag and Conventional  
Airfoil Sections. NACA Rep. No. 832; 1945.
2. Lindsey, W.F., Daley, Bernard N., and Humphreys, Milton D.:  
The Flow and Force Characteristics of Supersonic Airfoils  
at High Subsonic Speeds. NACA TN No. 1211, 1947.
3. Allen, H. Julian, Heaslet, Max. A., and Nitzberg, Gerald E.:  
The Interaction of Boundary Layer and Compression Shock and  
its Effect Upon Airfoil Pressure Distributions. NACA RM No.  
A7A02, 1947.

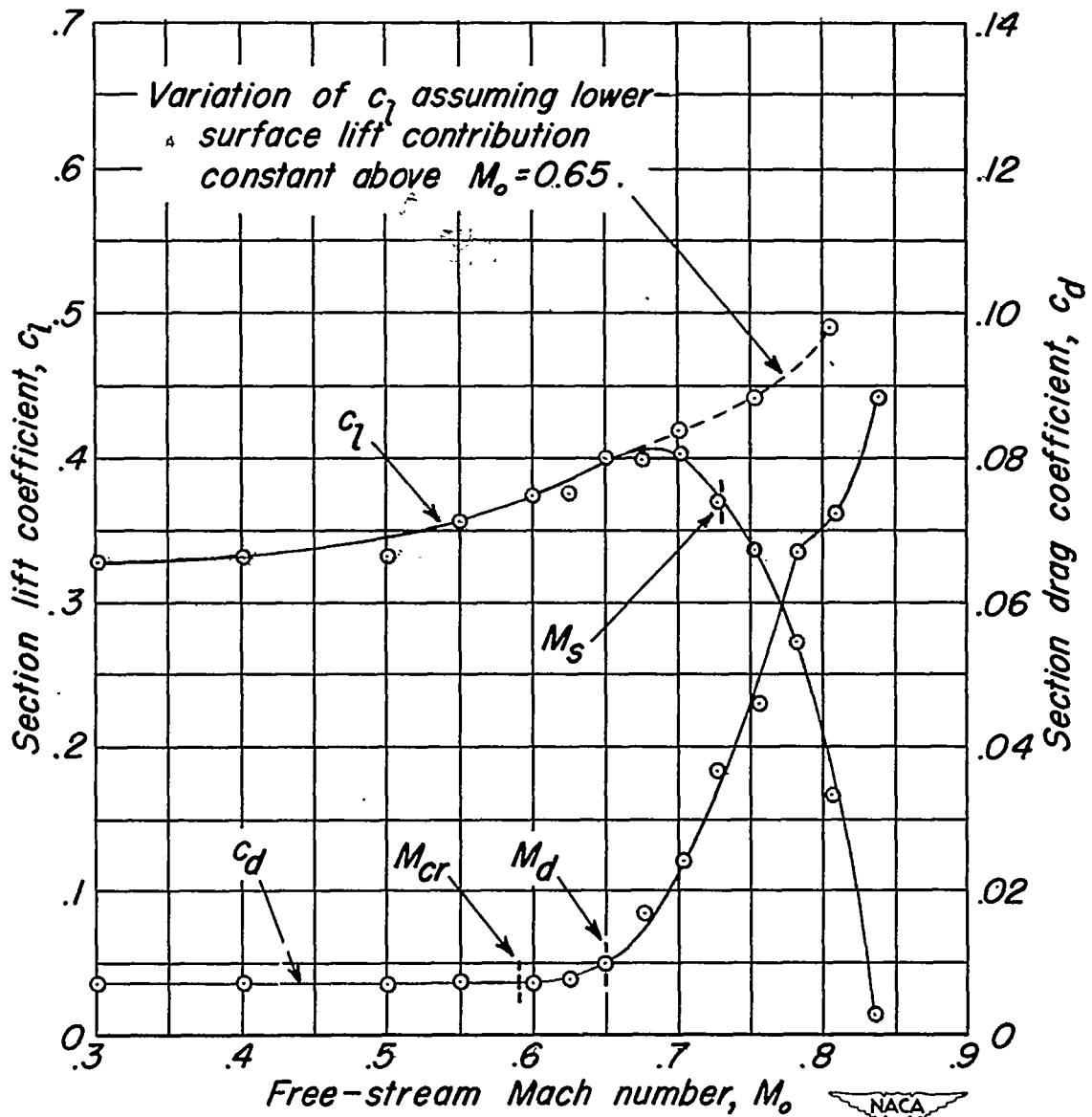
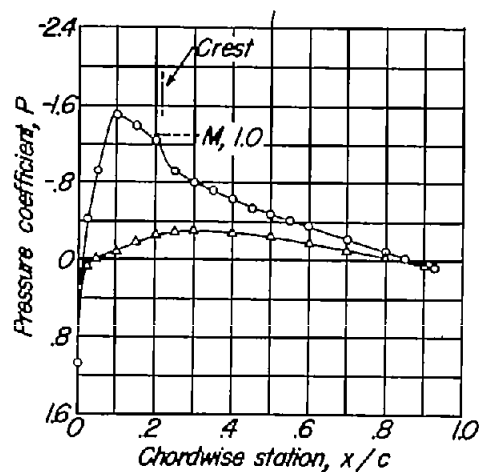
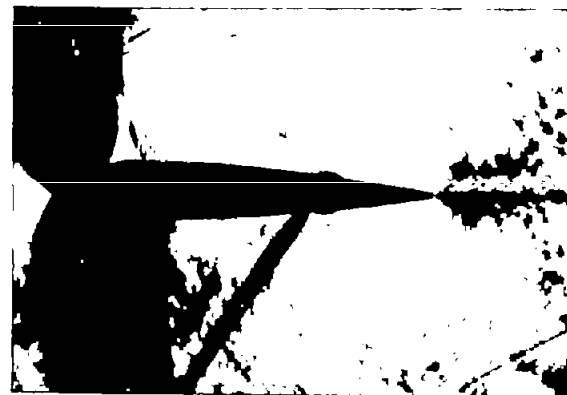
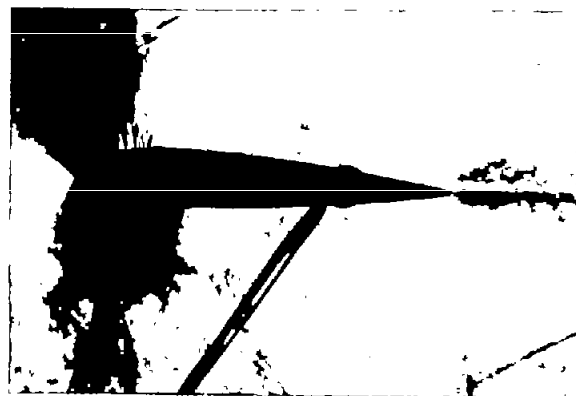
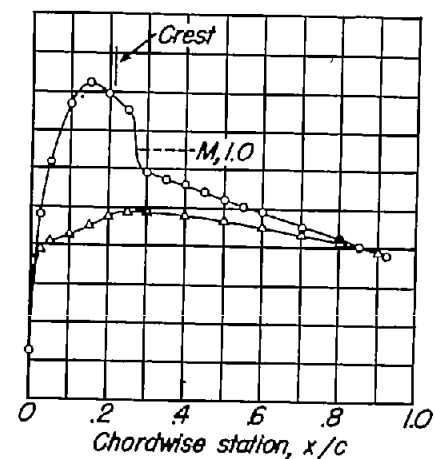


Figure 1.— Section lift and drag coefficients as functions of free-stream Mach number for NACA 23015 airfoil section at  $2^\circ$  angle of attack.





(a)  $M_o, 0.60$

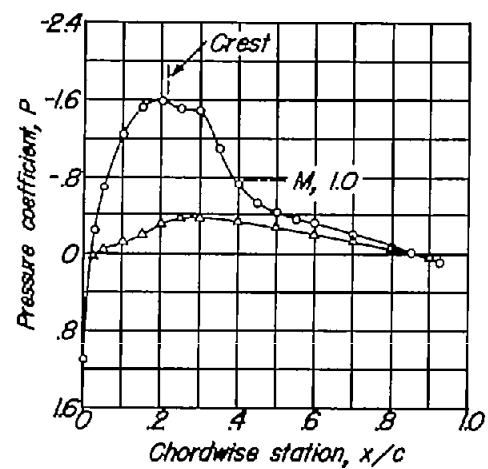


(b)  $M_o, 0.65$

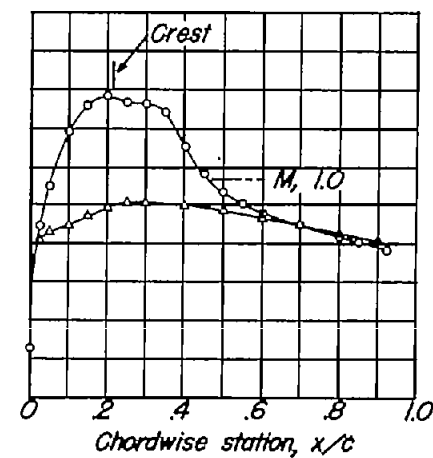


Figure 2.— Simultaneously obtained pressure distributions and schlieren photographs for NACA 23015 airfoil section;  $\alpha, 2^\circ$ .





(c)  $M_o, 0.70$



(d)  $M_o, 0.73$

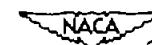
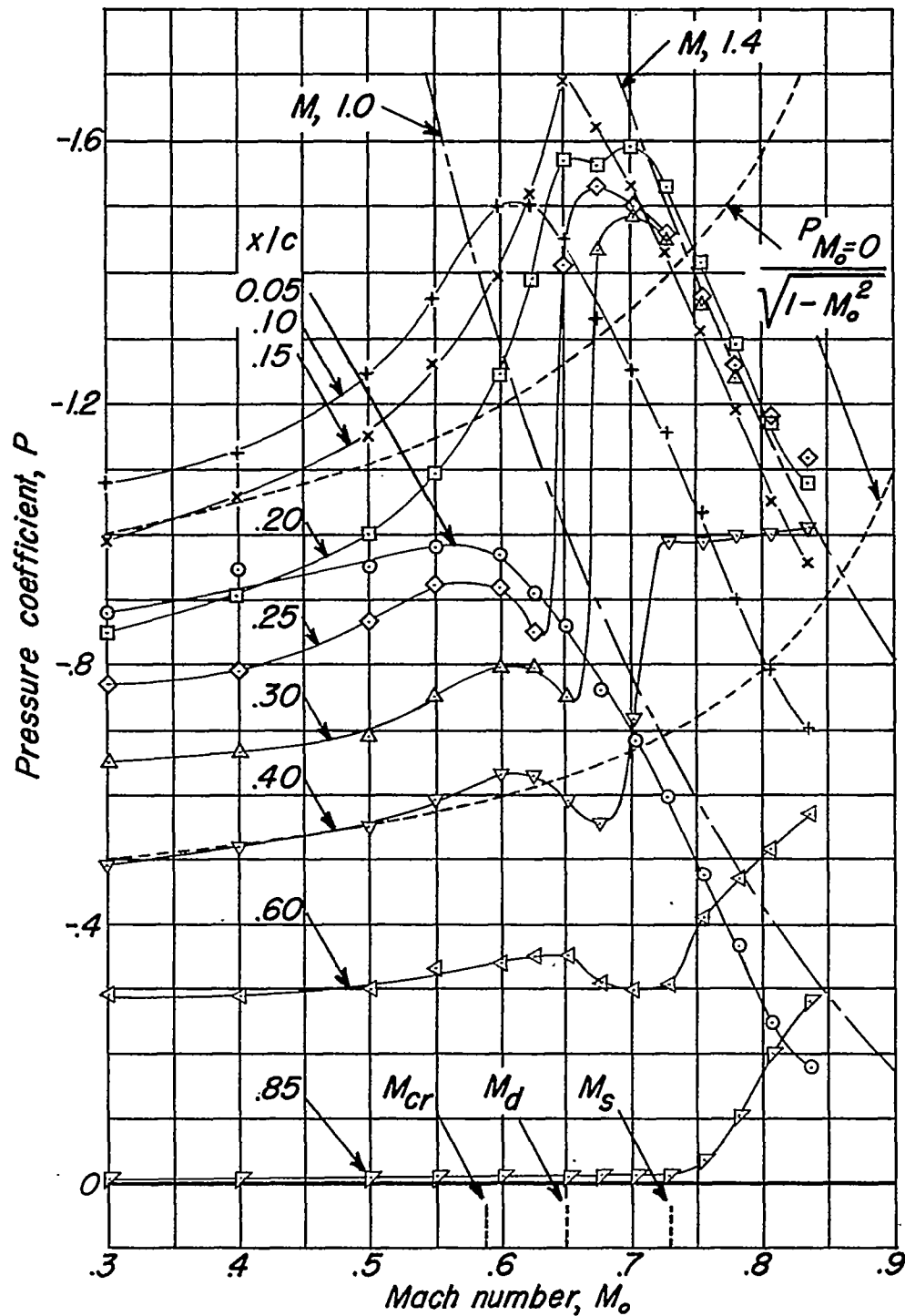


Figure 2.— Concluded.



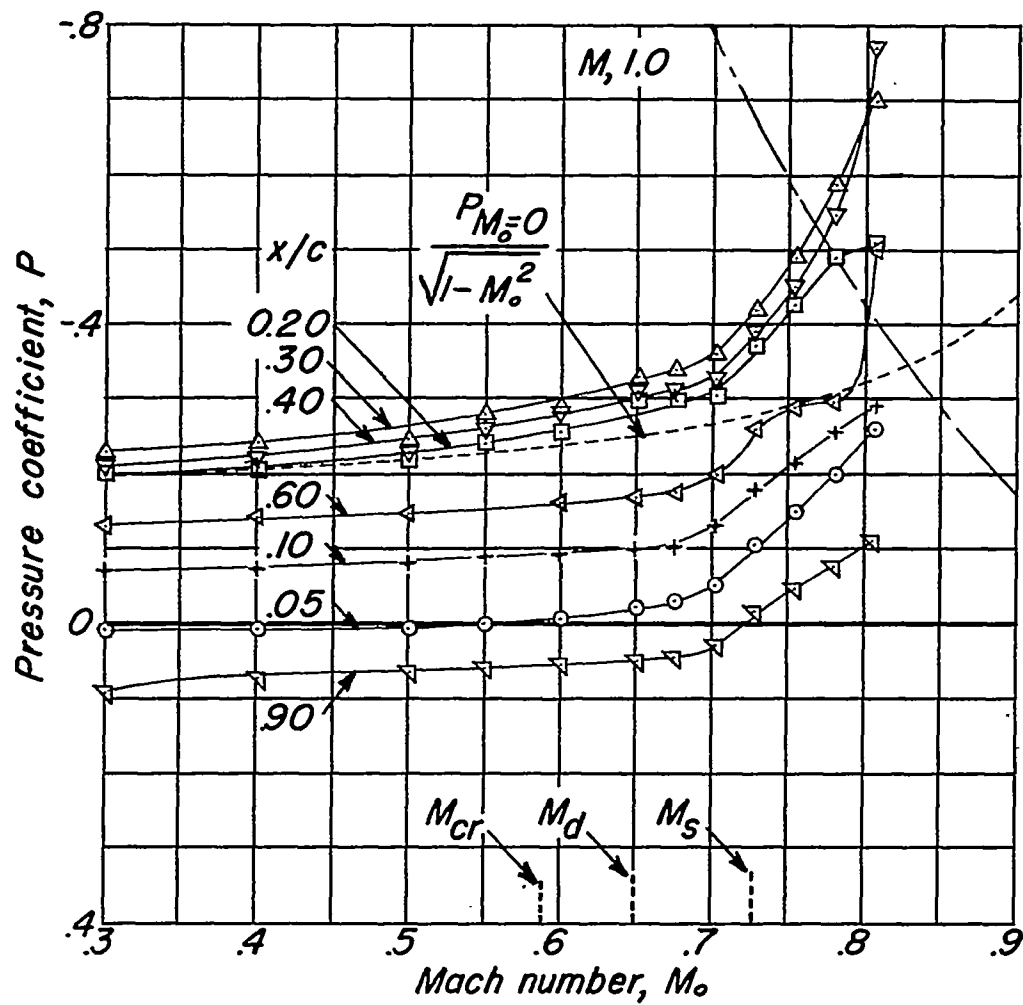




(a) Upper surface.



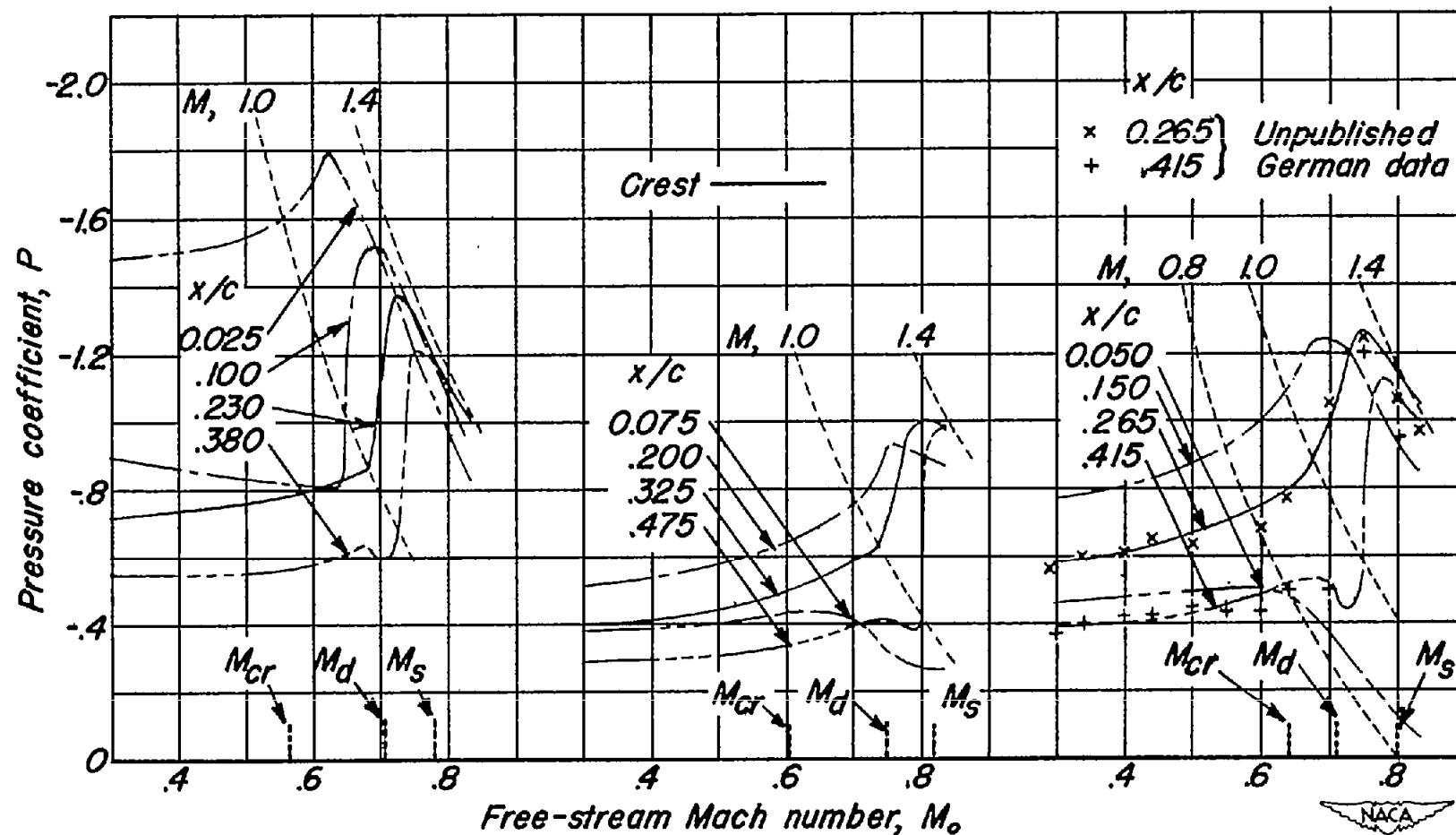
Figure 3.— Variation of pressure coefficient with Mach number at various chordwise stations of NACA 23015 airfoil section;  $\alpha, 2^\circ$ .



(b) Lower surface.

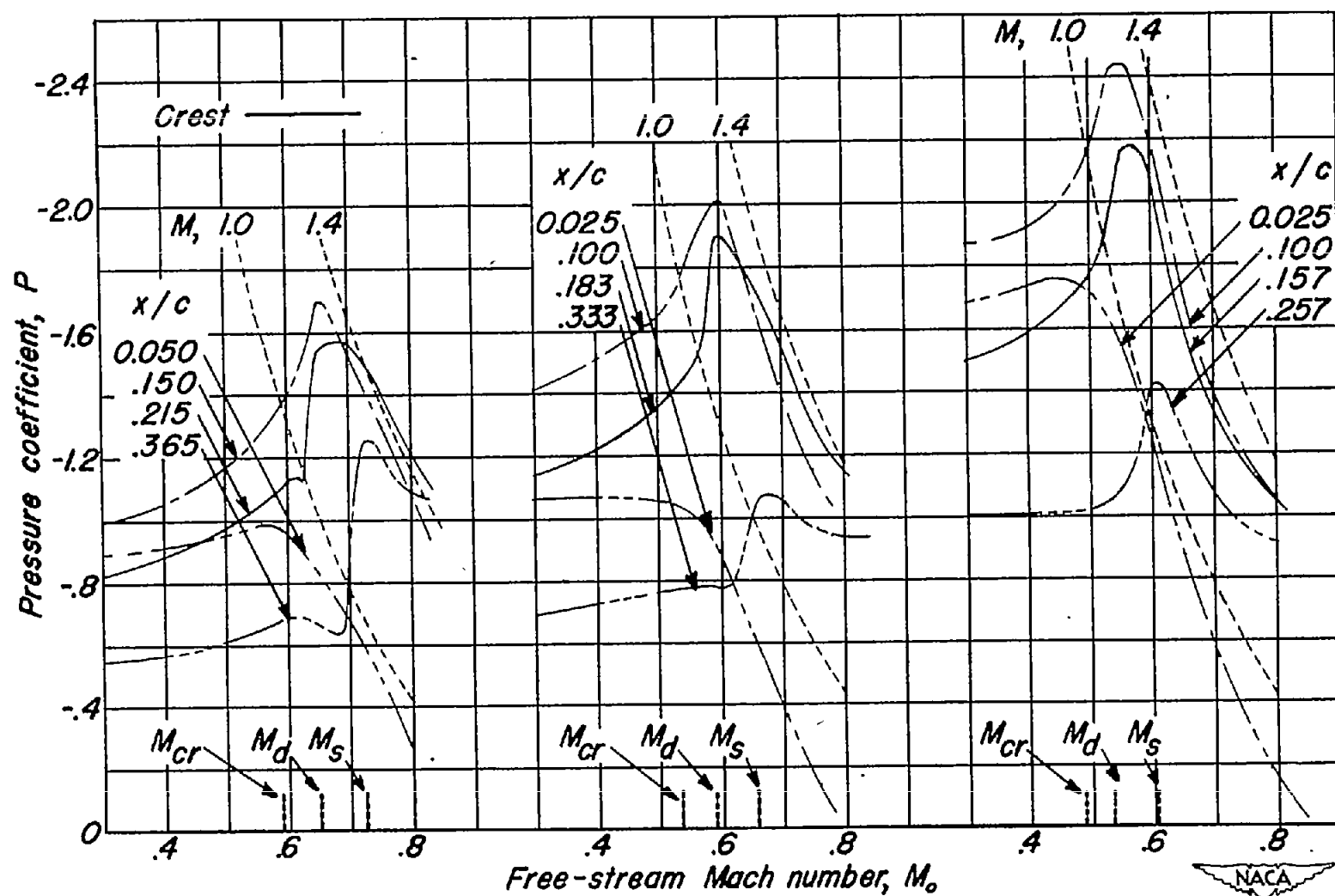


Figure 3.- Concluded.



(a)  $\alpha, -4^\circ$ ; lower surface. (b)  $\alpha, -2^\circ$ ; upper surface. (c)  $\alpha, 0^\circ$ ; upper surface.

Figure 4.- Pressure coefficient at various chordwise locations as a function of free-stream Mach number for NACA 23015 airfoil section.



(d)  $\alpha, 2^\circ$ ; upper surface. (e)  $\alpha, 4^\circ$ ; upper surface. (f)  $\alpha, 6^\circ$ ; upper surface.

Figure 4.- Concluded.

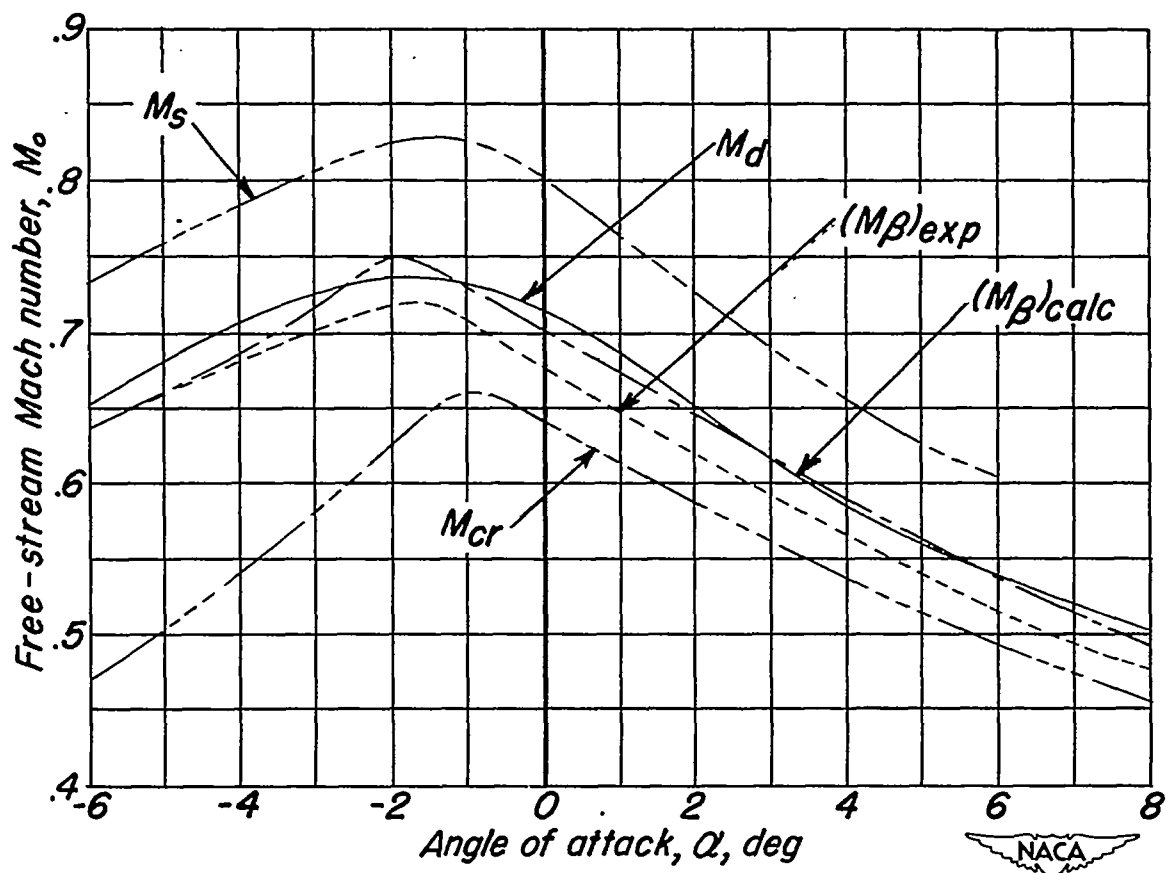
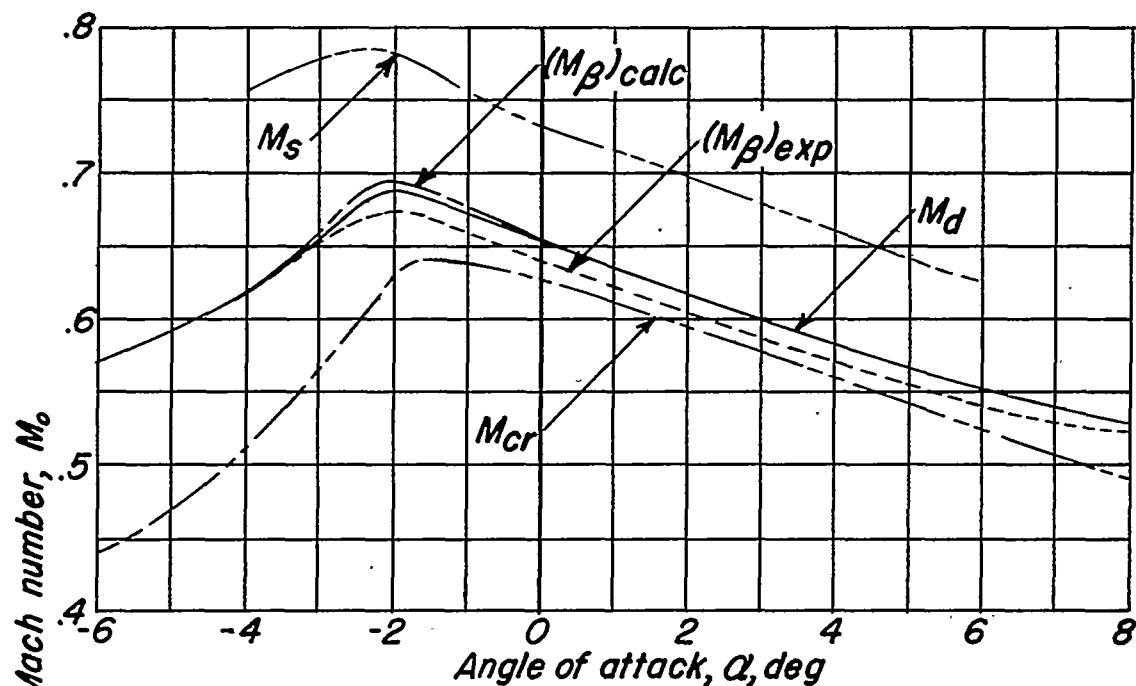
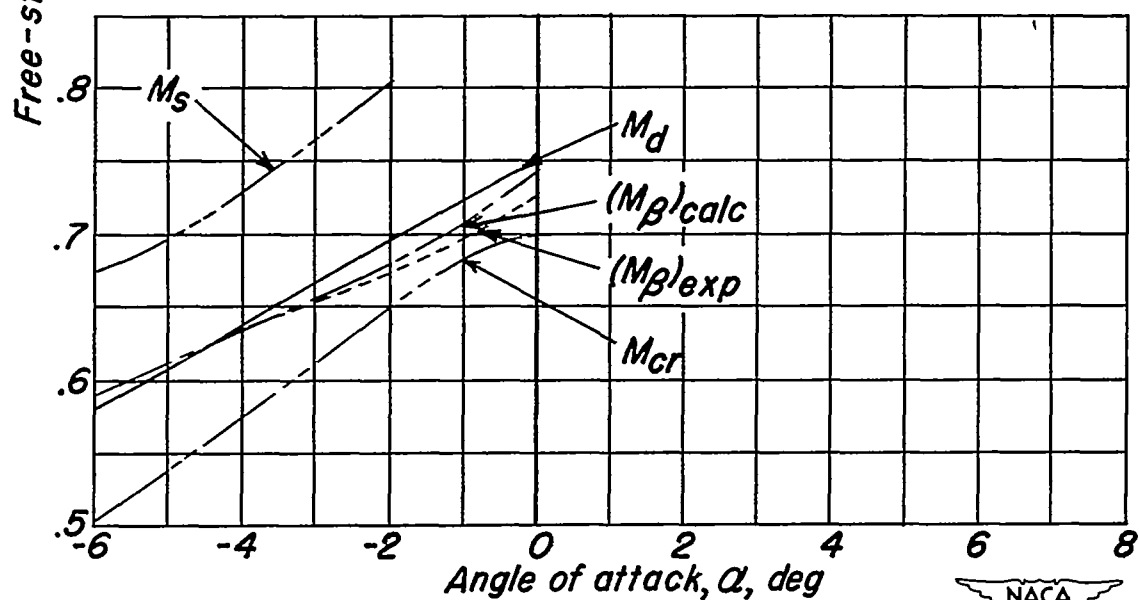


Figure 5.—Variation of critical, drag-divergence, and shock-stall Mach numbers with angle of attack for the NACA 23015 airfoil section.

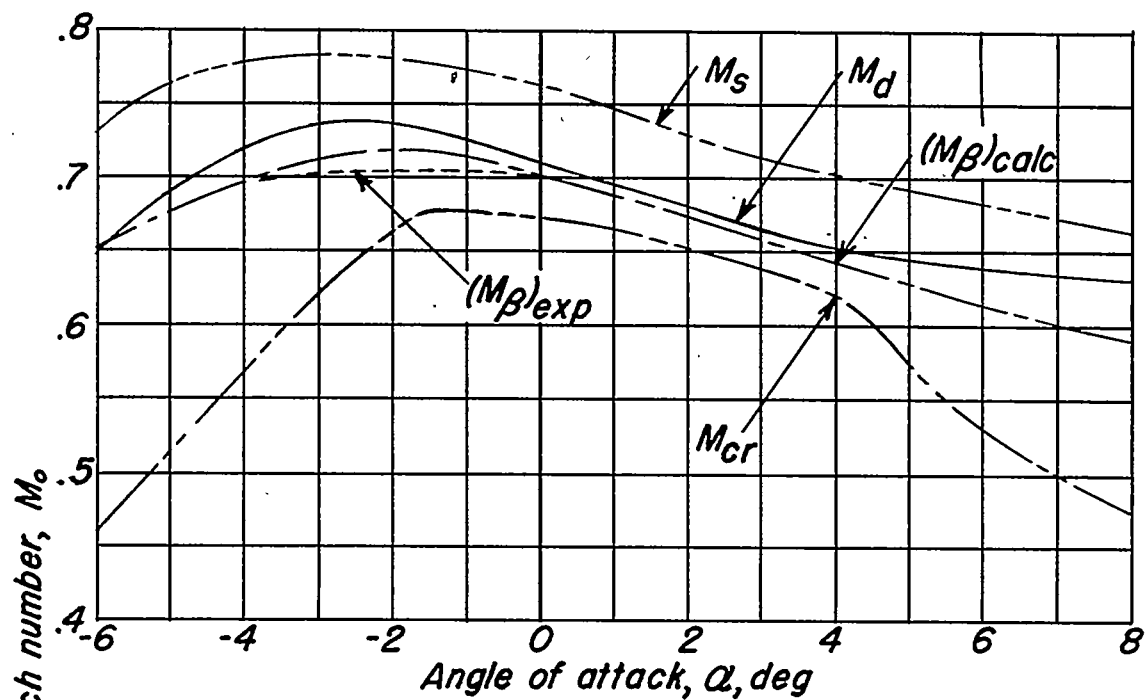


(a) Airfoil section, NACA 4415.

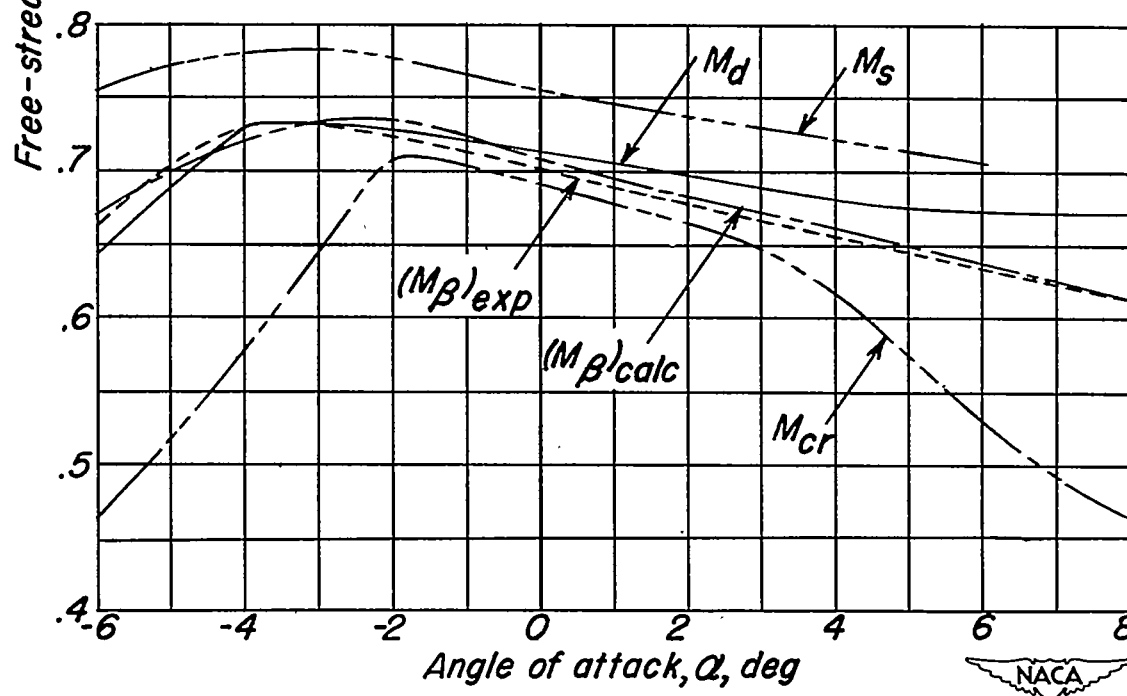


(b) Airfoil section, NACA 0015.

Figure 6.—Variation of critical, drag-divergence, and shock-stall Mach numbers with angle of attack for several NACA airfoil sections.



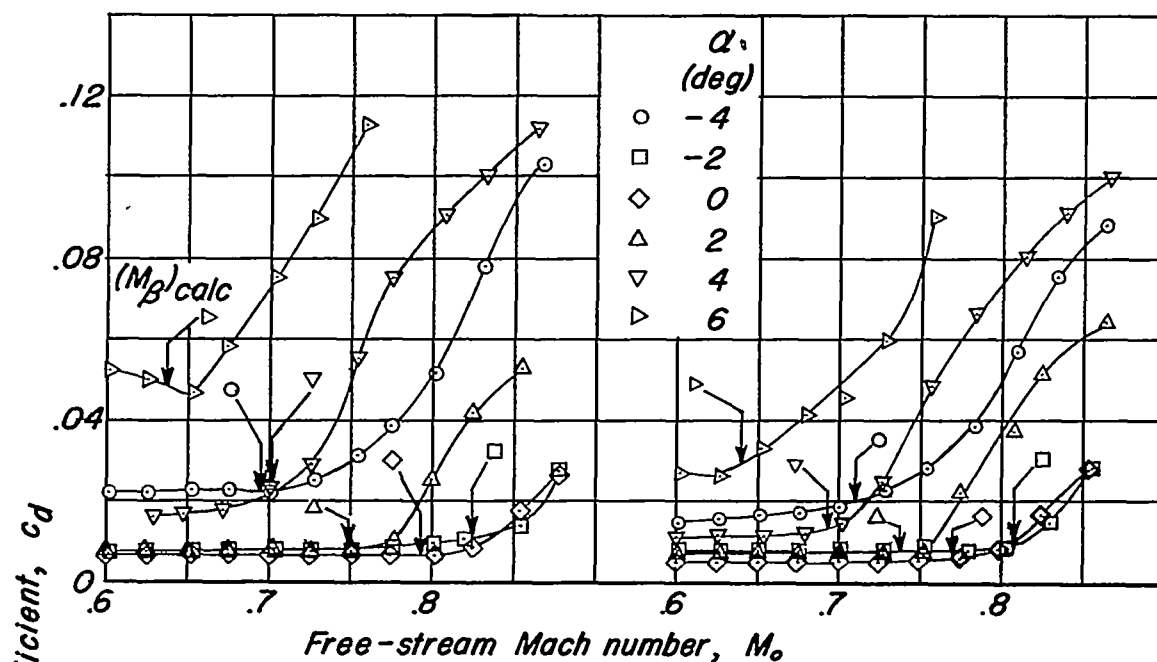
(c) Airfoil section, NACA 65<sub>2</sub>-215,  $a=0.5$ .



(d) Airfoil section, NACA 66,2-215,  $a=0.6$ .

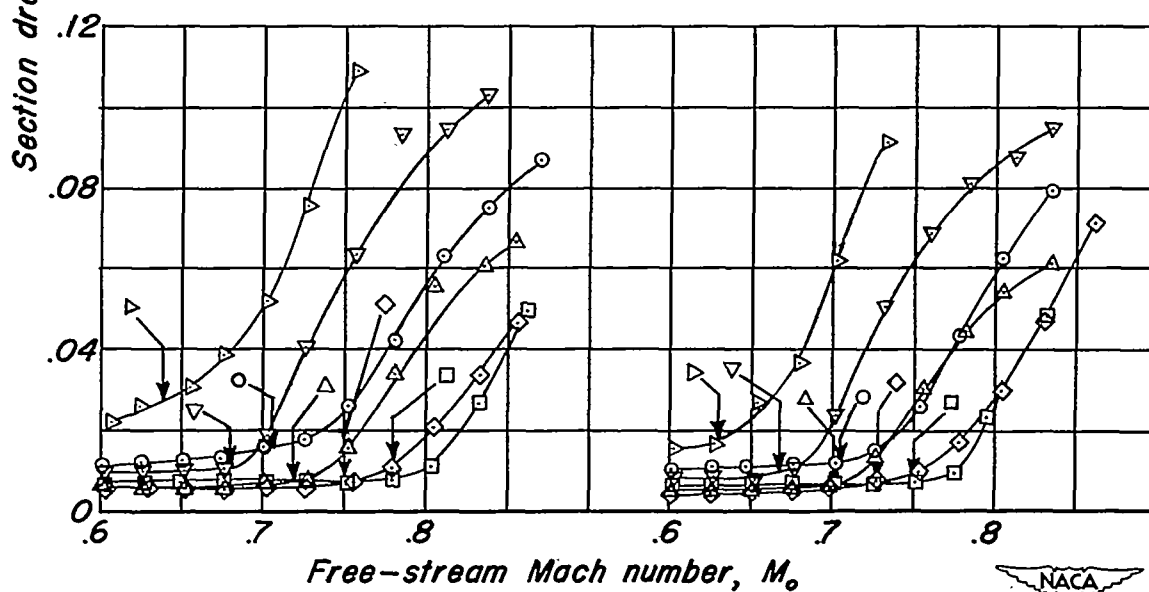
Figure 6.—Concluded.





(a) NACA 64,-206.

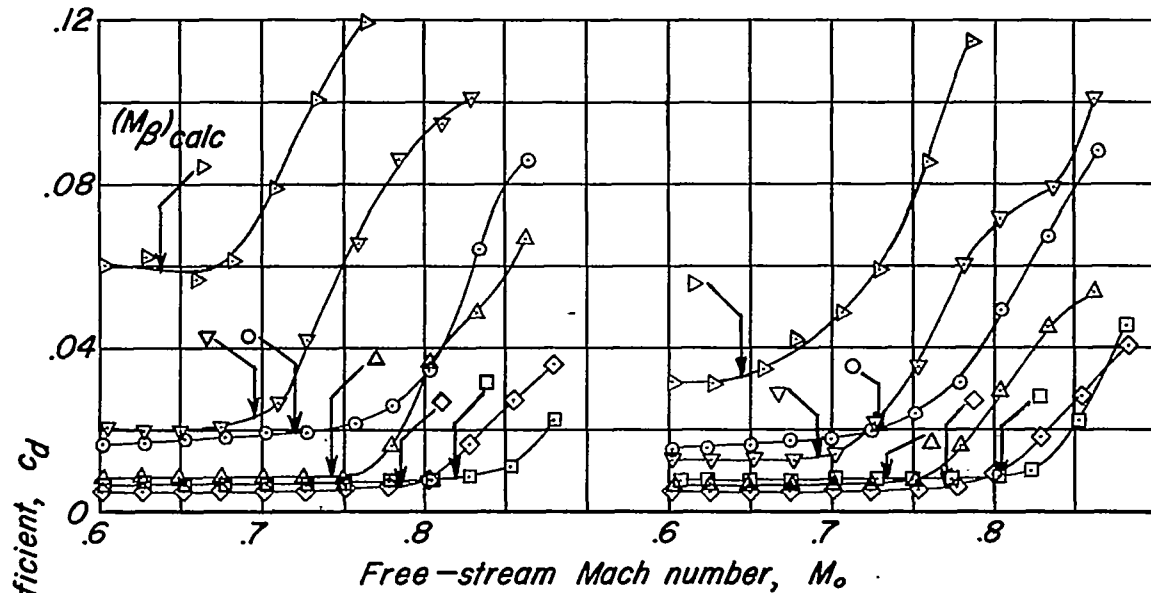
(b) NACA 64,-208.



(c) NACA 64,-210.

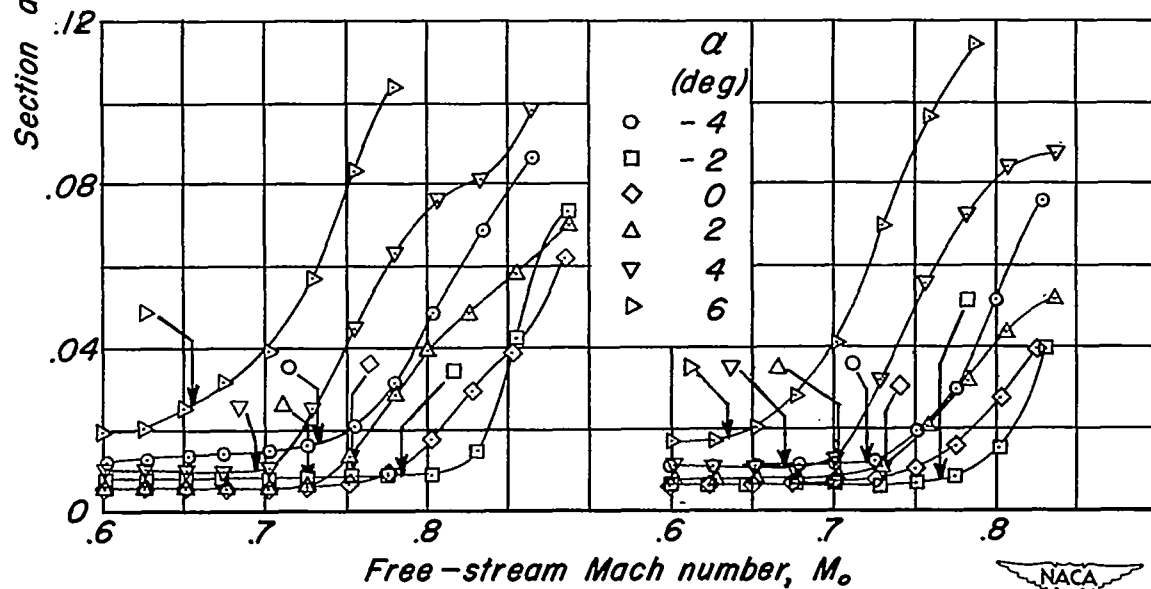
(d) NACA 64,-212.

Figure 7.- Calculated Mach number for occurrence of sonic velocity at airfoil crest and variation of section drag coefficient with Mach number for a variety of airfoil sections.



(e) NACA 65,-206.

(f) NACA 65,-208.



(g) NACA 65,-210

(h) NACA 65,-212.

Figure 7.- Continued.

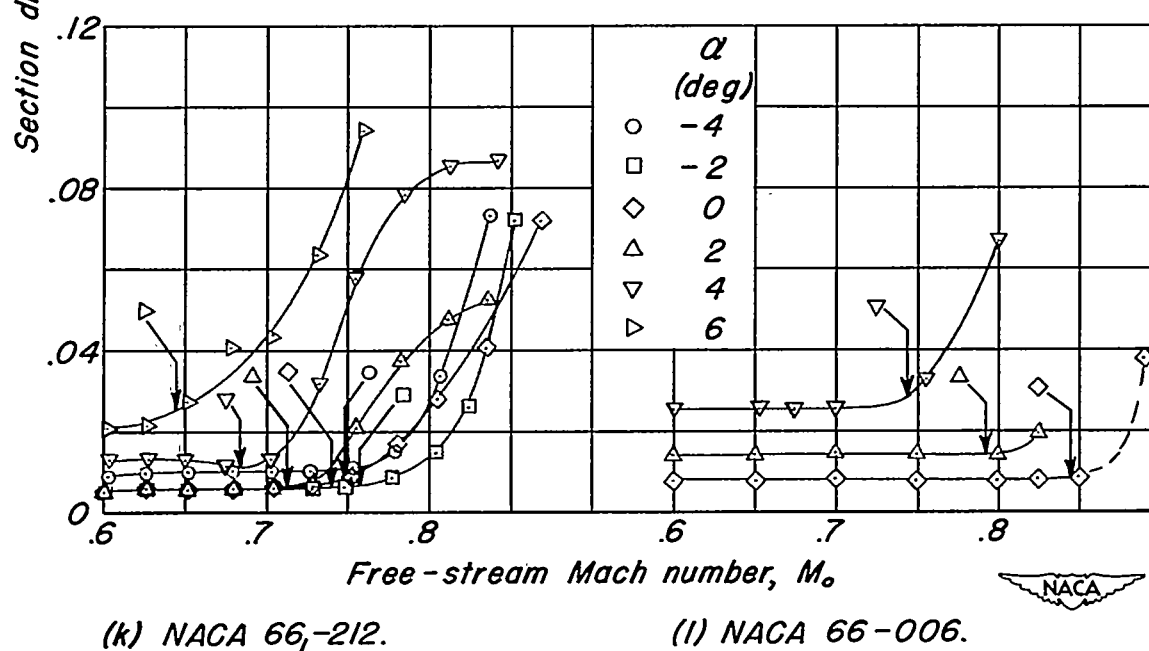
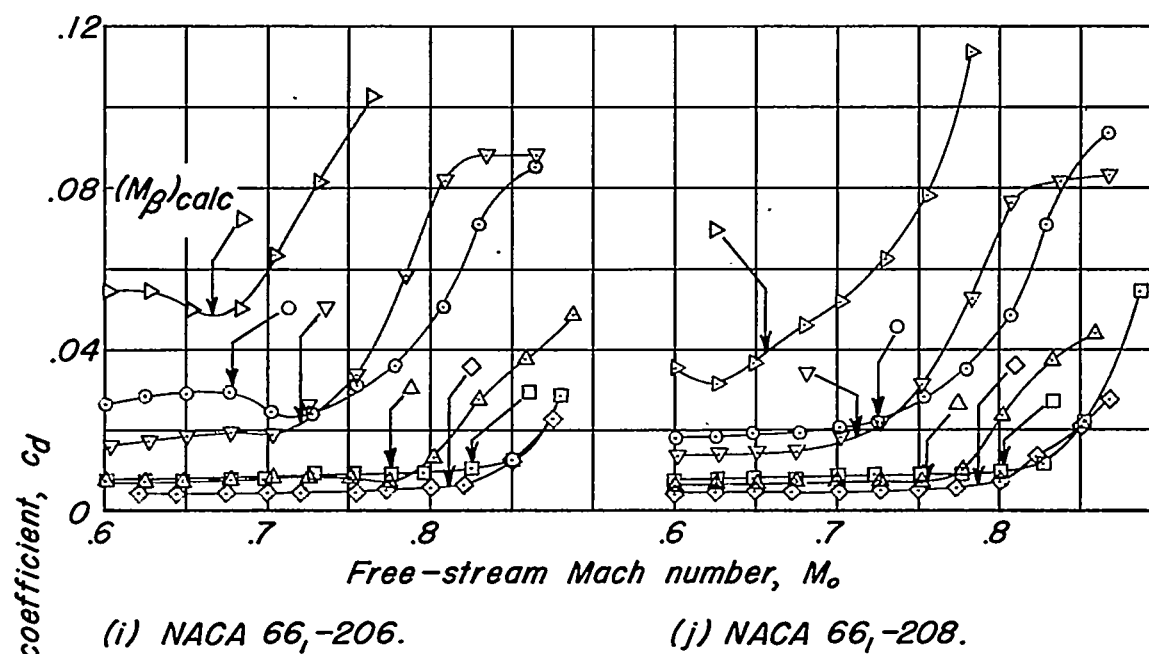
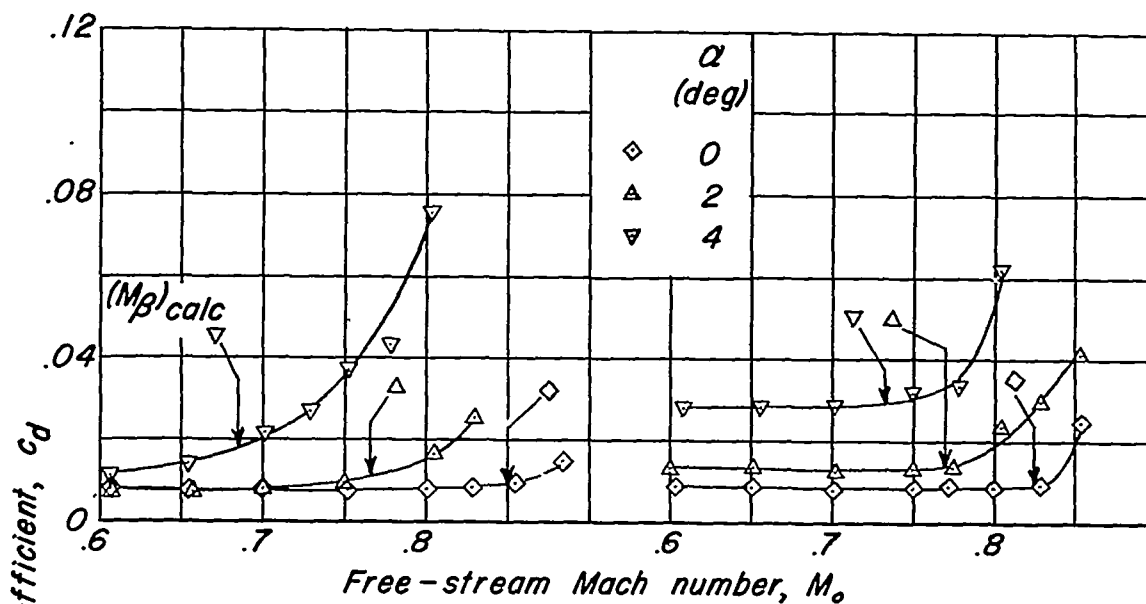
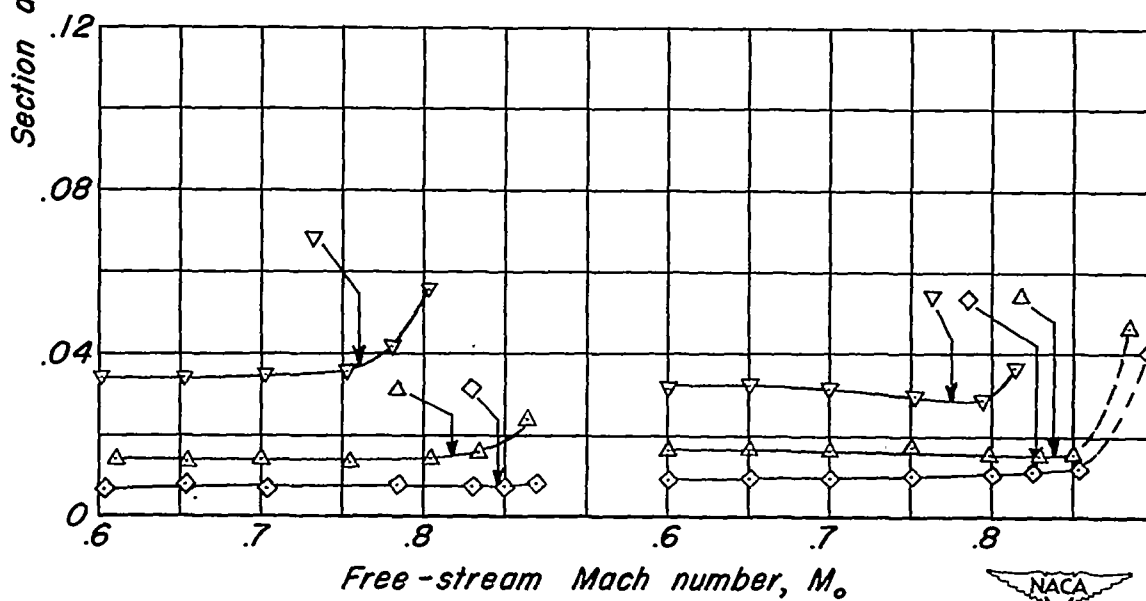


Figure 7.- Continued.



(m) NACA 0006.

(n) 2S-(30)(03)-(30)(03).



(o) 2S-(50)(03)-(50)(03).

(p) 2S-(70)(03)-(70)(03).

Figure 7.- Concluded.

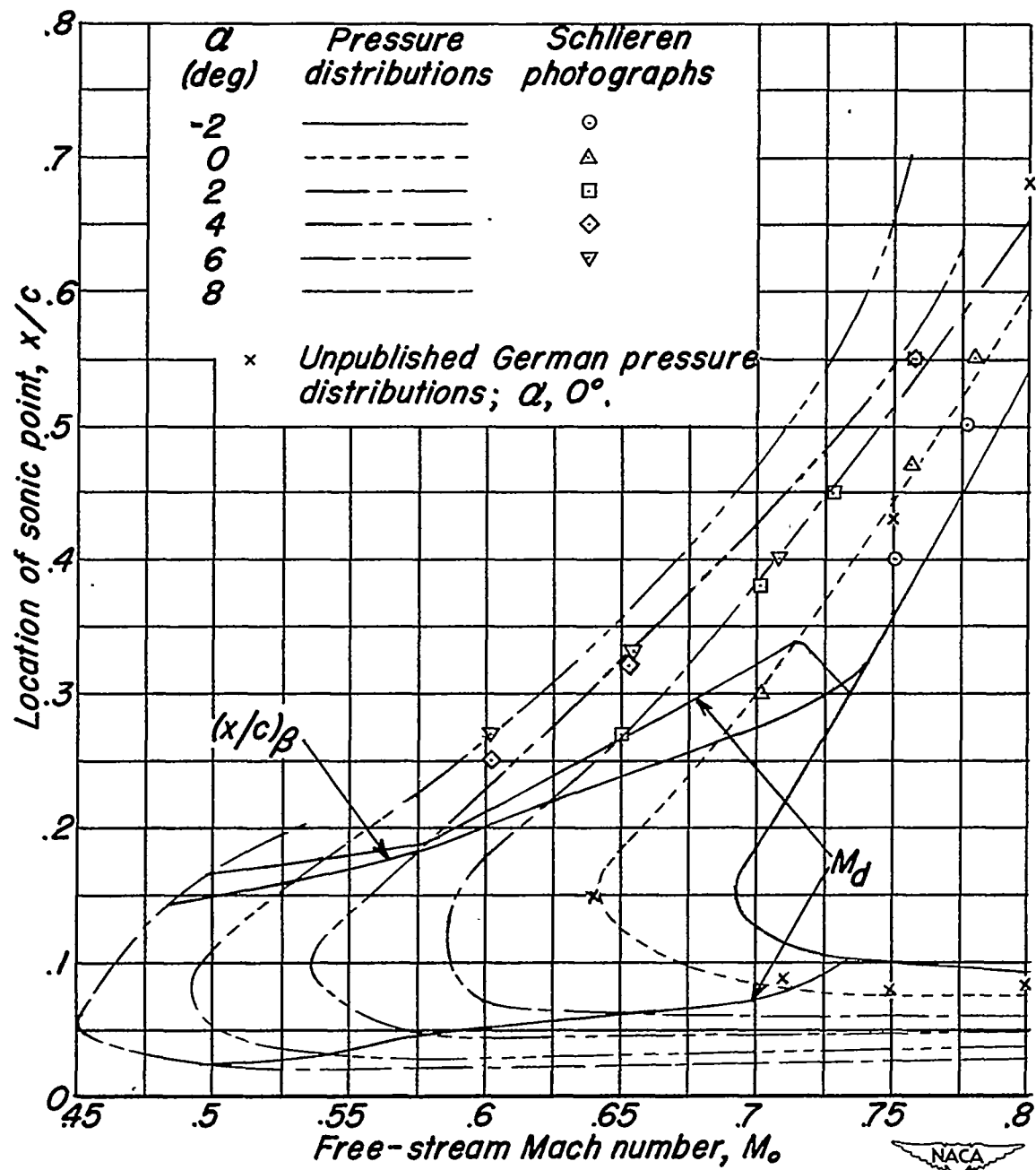


Figure 8.—Boundaries of supersonic region on upper surface of NACA 23015 airfoil section as a function of free-stream Mach number for various angles of attack.

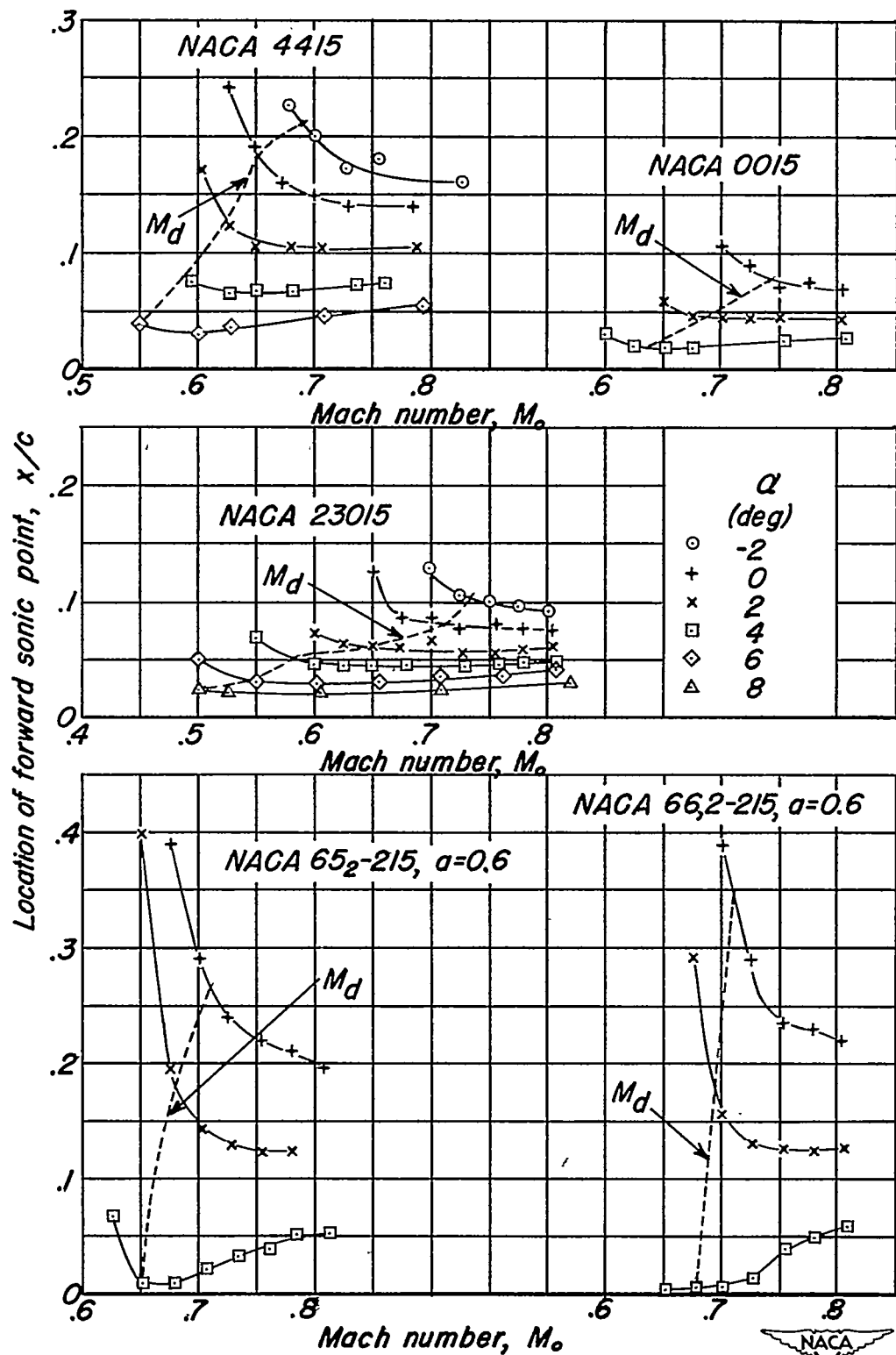


Figure 9.— Location of forward sonic point as a function of free-stream Mach number for several NACA airfoil sections.

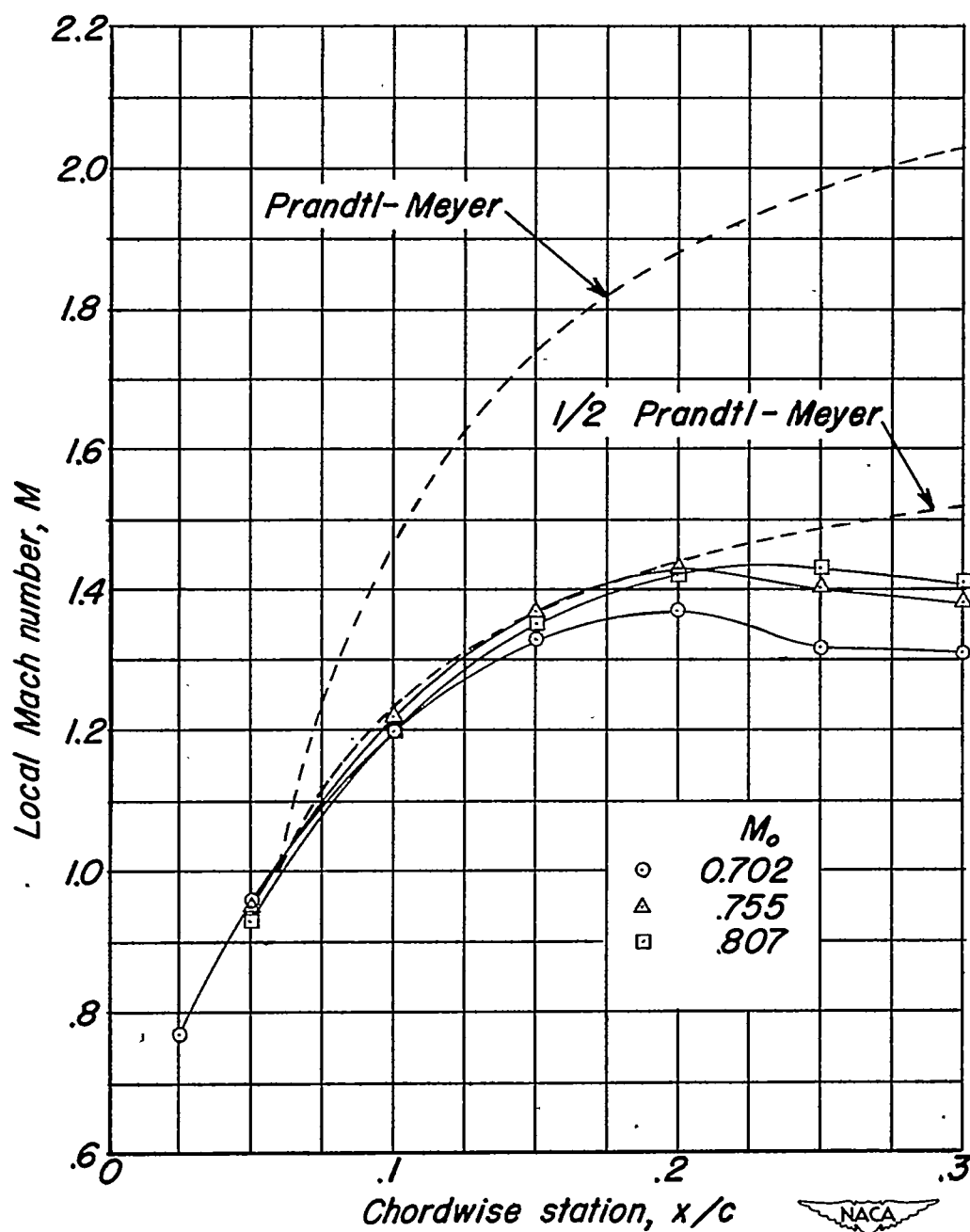


Figure 10.— Local Mach number distribution over upper surface of NACA 23015 airfoil section;  $\alpha$ ,  $2^\circ$ .

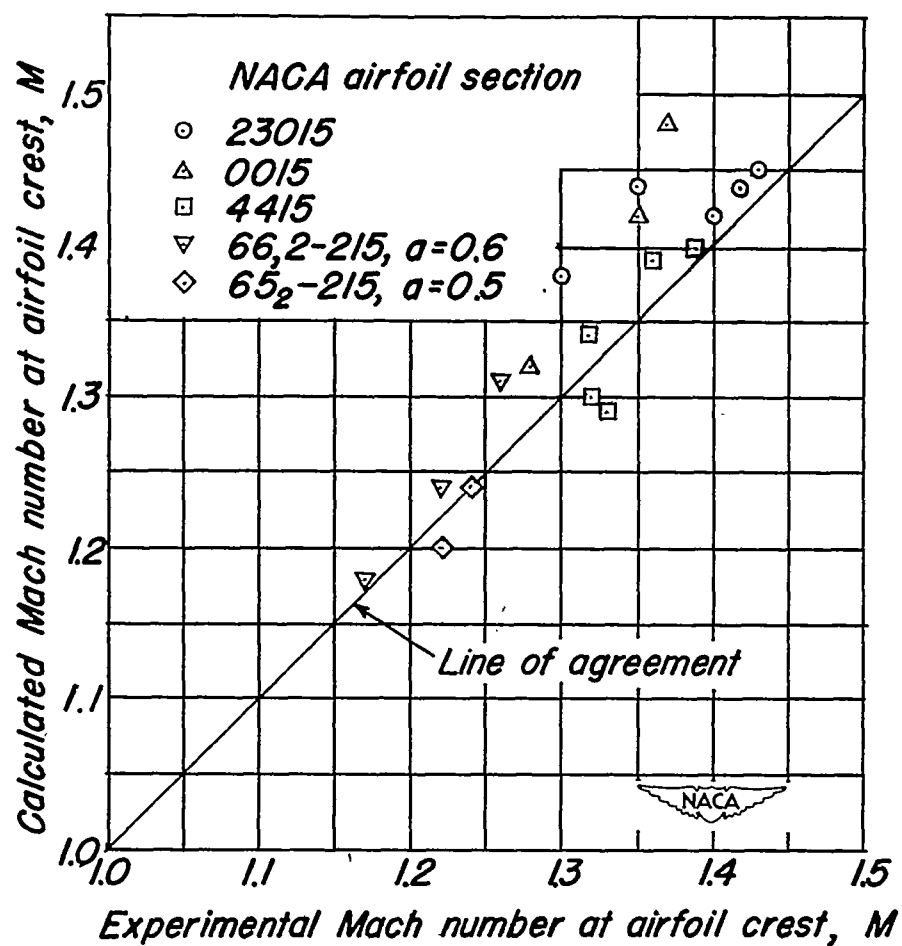


Figure 11.— Comparison of calculated and experimental values of local Mach number at airfoil crest for several NACA airfoil sections.